

Two new high-energy γ -ray blazar candidates

R. Campana,¹★ A. Maselli,² E. Bernieri³ and E. Massaro^{4,5}

¹INAF/IASF-Bologna, via Piero Gobetti 101, I-40129 Bologna, Italy

²INAF/IASF-Palermo, via Ugo La Malfa 153, I-90146 Palermo, Italy

³INFN-Sezione di Roma Tre, via della Vasca Navale 84, I-00146 Roma, Italy

⁴INAF/IAPS, via Fosso del Cavaliere 100, I-00133 Roma, Italy

⁵In Unam Sapientiam, Piazzale A. Moro 2, I-00185 Roma, Italy

Accepted 2016 November 17. Received 2016 November 17; in original form 2016 August 22

ABSTRACT

We report the detection of two new γ -ray sources in the *Fermi*-Large Area Telescope sky (Pass 8) at energies higher than 20 GeV and confirmed at lower energies, using a source detection tool based on the Minimum Spanning Tree algorithm. One of these sources, at a Galactic latitude of about -4° , is a new discovery, while the other was previously reported above 50 GeV in the 2FHL catalogue. We searched for archival multiwavelength data of possible counterparts and found interesting candidates. Both objects are radio sources and their *Wide-field Infrared Survey Explorer* infrared colours are typical of blazars. While, for the former source, no optical spectra are available, for the latter, a puzzling optical spectrum corresponding to a white dwarf star is found in the 6dF data base. We discuss the spectral energy distributions of both sources and possible interpretations.

Key words: methods: data analysis – gamma-rays: galaxies – gamma rays: general.

1 INTRODUCTION

The entire γ -ray sky in the 0.03 to >300 GeV band is continuously observed by the *Fermi*-Large Area Telescope (LAT) experiment (Atwood et al. 2009) since 2008 August. To date, the *Fermi* collaboration has published three catalogues of sources detected above 100 MeV, the most recent of which (3FGL catalogue; Acero et al. 2015) is based on the first 4 yr of data and two catalogues of high-energy sources above 10 GeV (1FHL; Ackermann et al. 2013) and 50 GeV (2FHL; Ackermann et al. 2016), the latter covering a time interval of 80 months. In addition, some specific catalogues for selected classes of objects such as pulsars (Abdo et al. 2013) and supernova remnants (Acero et al. 2016) have also been published. The continuous increase of observational data, in addition to the improved new data processing and instrumental response functions (Pass 8), has enriched the quality of the *Fermi*-LAT γ -ray sky and has raised its capability to detect new sources.

In a series of papers, we successfully applied a tool based on the Minimum Spanning Tree (MST) algorithm (Campana et al. 2008, 2013) to search for photon clusters in the γ -ray sky at Galactic latitudes higher than 25° and to associate them with known blazars or candidates within an angular distance of 6 arcmin (Campana et al. 2015; Campana, Massaro & Bernieri 2016a,b,c). In this paper, we report the detection, with the same MST clustering method, of two new high-energy γ -ray sources found while analysing the *Fermi*-LAT Pass 8 sky in regions below the previous

Galactic latitude limit. The new sources were first detected applying the MST analysis at energies higher than 20 GeV and then confirmed by similar analysis at lower energies. One of these clusters was found to coincide with the source 2FHL J1944.9–2144 previously detected above 50 GeV (Ackermann et al. 2016), but never reported at lower energies.

We completed the analysis of these two sources by means of the *Fermi* Science Tools¹, based on the Maximum Likelihood (ML) method, to obtain count maps, light curves (LC) and Test Statistics (TS) values. As a final step, we searched in data archives and in the literature for possible counterparts at lower energies, from the radio to the soft X rays, and discussed their properties to confirm their possible blazar nature, as well as some open issues for one of them.

2 MST DETECTION OF γ -RAY CLUSTERS

MST is a topometric cluster-finding algorithm that exploits the pattern of ‘connectedness’ of the detected photons, treated as the nodes in a graph, where the edges are the angular distances connecting them. The advantage of MST is the capability to quickly find potential γ -ray sources by examining only the incoming directions of the photons, regardless of their energy distribution. In the specific application of MST to the γ -ray sky, we defined (and successfully tested on simulated and real fields) various selection parameters, useful to assess the significance of the detected clusters and therefore their possible nature as genuine astrophysical sources

* E-mail: campana@iasfbo.inaf.it

¹ <http://fermi.gsfc.gov/ssc/data/analysis/software>

Table 1. Coordinates and main properties of MST clusters detected at energies higher than 20 GeV in the first considered region. The first pair of columns gives the J2000 coordinates of the MST clusters, while the second pair the Galactic coordinates. The other columns give the number of photons, the clustering factor, the magnitude, the median and the maximum radii (i.e. the radii from the cluster centroid coordinates that contain 50 per cent and all the cluster photons, respectively) and the angular separation from the 3FGL source. The last two rows report the cluster parameters detected in a narrower field but with $E > 10$ GeV and $E > 3$ GeV (see the text for details).

MST cluster	RA J2000	Dec. J2000	l ($^\circ$)	b ($^\circ$)	n	g	M	R_m ($^\circ$)	R_{\max} ($^\circ$)	$\Delta\theta$ (arcmin)	Notes
MST 0747–3313	116.8212	–33.1776	248.4199	–4.0029	7	6.612	46.284	0.027	0.076	0.6	3FGL J0747.2–3311
MST 0757–3728	119.3012	–37.4768	253.1631	–4.4466	14	2.483	34.759	0.181	0.385		
MST 0954–5741	136.2318	–57.6689	276.1837	–7.0924	13	3.683	47.880	0.089	0.224	3.9	3FGL J0904.8–5734
MST 0757–3728	119.2832	–37.4920	253.1687	–4.4668	22	3.180	69.950	0.084	0.342		
MST 0757–3728	119.2893	–37.5216	253.1967	–4.4779	22	2.686	59.081	0.061	0.136		

(Campana et al. 2008; Massaro et al. 2009; Campana et al. 2013). In particular, we found that the cluster magnitude M is a very good indicator of the detection significance; it is defined as $M = ng$, where n is the number of photons in a cluster and g is the clustering degree, i.e. the ratio of the mean edge length in the cluster to the mean value Λ_m in the field. As shown by Campana et al. (2013), in regions with a Galactic latitude high enough to have a rather uniform and not very dense background, M values higher than 20 correspond to significance values close to and generally higher than four standard deviations. The centroid coordinates, obtained by computing a weighted mean of the photons' coordinates (see, for details, Campana et al. 2013), give an indication if a cluster is compatible with a γ -ray source.

Once detected with the MST algorithm, the clusters can be further analysed with other well-recognized statistical methods, such as the ML (Mattox et al. 1996), in order to obtain an independent evaluation of their statistical significance and to study the time and energy properties of the corresponding source. In this sense, the MST method has been already applied to obtain lists of seed clusters for the 1FGL and 2FGL *Fermi*-LAT catalogues (Abdo et al. 2010; Nolan et al. 2012).

In this work, we have considered all the data collected in 7 yr by *Fermi*-LAT, from 2008 August 04 to 2015 August 04, both in a region close to the Galactic equator not distant from the very bright Vela pulsar and in two intermediate Galactic latitude belts ($14^\circ < |b| < 26^\circ$). Pass 8 data were filtered using the standard LAT Science Tools routines `gtselect` and `gtmktime` with standard cuts on the zenith angle and on the rocking angle to limit contamination from the bright Earth limb.

3 NEW MST PHOTON CLUSTERS

As mentioned before, in our previous works, we limited our analysis of the γ -ray sky at Galactic latitudes $|b| > 25^\circ$ to avoid large background inhomogeneities. In a subsequent study, we started to extend MST cluster search to regions closer to the Galactic belt, but considering higher selection thresholds to reduce the number of fake detections. Two interesting clusters were found in these searches and their main properties are described in the following.

3.1 The cluster MST 0757–3728

We analysed a $38^\circ \times 4^\circ$ region bounded by the Galactic coordinates $242^\circ < l < 280^\circ$, $-12^\circ < b < -4^\circ$ in the 20–300 GeV energy range. Adopting a severe selection length $\Lambda_{\text{cut}} = 0.6 \Lambda_m$ (see Campana et al. 2008, 2013, for details) and applying the further threshold $M \geq 25$, we found only three clusters whose coordinates and MST parameters are given in Table 1. The coordinates of two

clusters are very close to those of 3FGL sources within a few arcminutes, while the third one, MST 0757–3728, has been never reported before. A refined search for this last source in a narrower strip ($-7.5 < b < -3.5$) at energies higher than 10 GeV gave a much more significant detection (see Table 1) with only slight changes of the centroid coordinates but compatible with the previous ones. A further analysis at $E > 3$ GeV gave a cluster with 22 photons but again with a highly significant magnitude (last line in Table 1) confirming the robustness of the detection.

False colour images of the photon density are given in the two upper panels of Fig. 1: note how for $E > 10$ GeV (right-hand panel), the photon cluster is readily apparent and its size is very similar to those of 3FGL sources, while for $E > 3$ GeV (left-hand panel), it is still detectable but the local background is much higher. No correspondence for this cluster was found in the 2nd LAT Pulsar Catalogue (Abdo et al. 2013) and in the LAT Supernova Remnants Catalogue (Acero et al. 2016).

3.2 The cluster MST 1945–2143

MST analysis was also applied to events in the 10–300 GeV energy range in two belts with Galactic coordinates in the range $14^\circ < |b| < 26^\circ$ and applying, as in the previous case, the threshold $M \geq 25$. Of the 294 resulting clusters, 231 are in the 3FGL catalogue. Furthermore, after a more robust filtering with $g > 3.5$ in order to reduce the possibility of selecting extended features, the number of new clusters decreased to 23. The one with the highest M among them (centroid coordinates RA = 296:2141 and Dec. = $-21:7190$; $l = 18:5665$; $b = -21:0826$) has 20 photons and $M = 161.6$, much higher than in the other cases and typical of safely confirmed γ -ray sources. We found that a source at a very close position (1.9 arcmin from the cluster centroid coordinates) was already reported in the more recent 2FHL catalogue as 2FHL J1944.9–2144, but no analysis on its possible counterparts was presented.

We performed a refined MST analysis in a small sky region $8^\circ \times 8^\circ$ wide at different energies and dividing the entire data set into three equal time intervals, each of length 28 months. The results using the two lower energy thresholds $E > 3$ GeV and $E > 10$ GeV are reported in Table 2 and clearly show that the source was brighter in the last interval (III). During interval I, the source is well detected at $E > 3$ GeV, while using the $E > 10$ GeV data, the cluster has a lower significance. In interval II, the cluster significance was at the same level of background fluctuations for both values of the lower energy thresholds. There is no doubt that it should also be highly variable and not detectable in the observation periods covered by other *Fermi*-LAT catalogues.

Photon density maps are given in the lower panels of Fig. 1: note that for $E > 10$ GeV (right-hand panel), the photon cluster is very

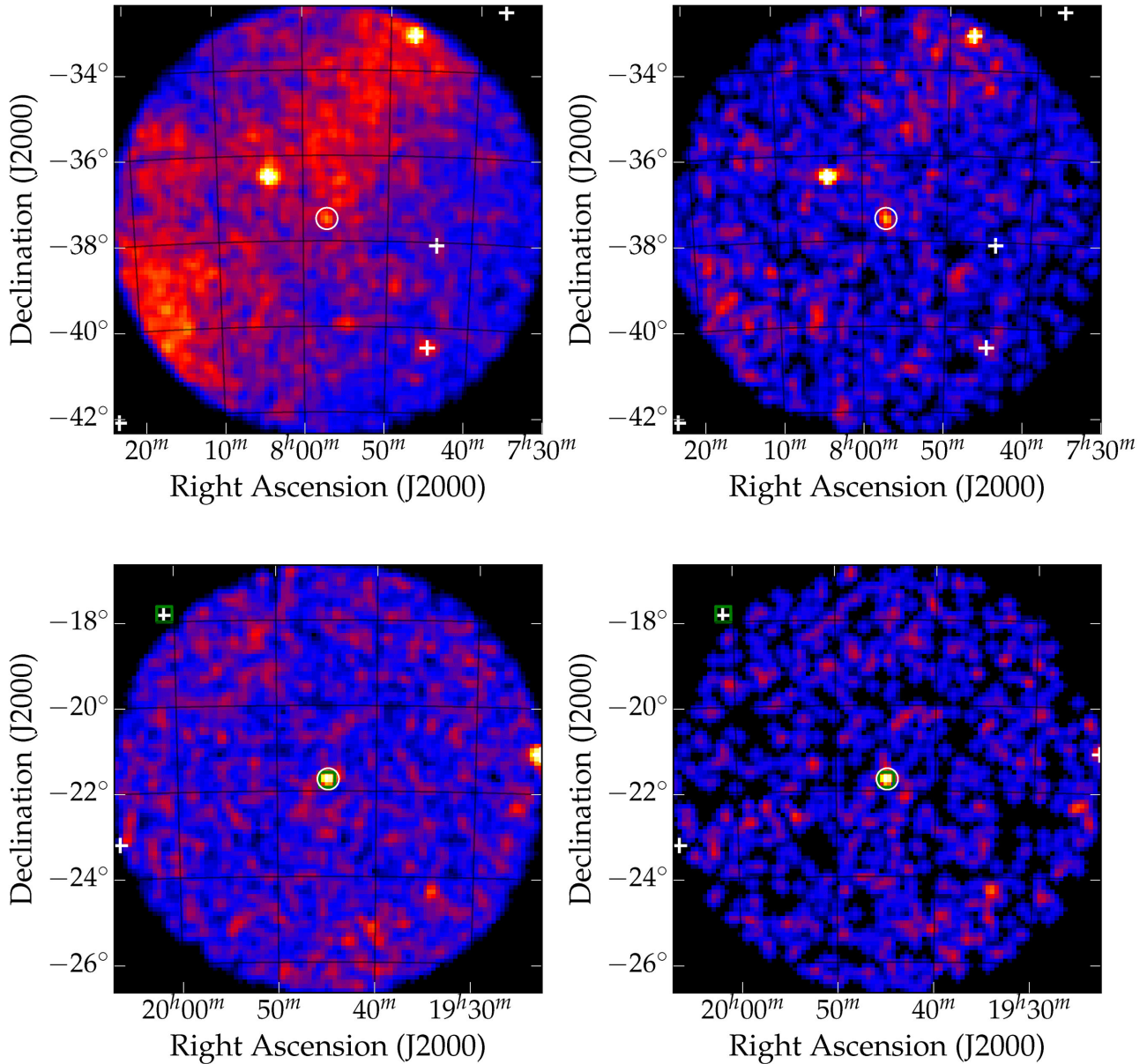


Figure 1. Upper panels: false colour count images in equatorial coordinates at energies higher than 3 (left) and 10 GeV (right) of the sky region centred at the cluster MST 0757–3728. Lower panels: the same for the sky region centred at the cluster 2FHL J1944.9–2144. For all the count maps, the radius of the considered circular region is 5° . White cross and green square symbols indicate the positions of 3FGL and 2FHL sources, respectively, while the white circles correspond to the MST cluster centroid coordinates.

well apparent and that for $E > 3$ GeV (left-hand panel), it remains still detectable despite a higher local background.

4 ML ANALYSIS AND LC

We verified the significance of both these clusters by means of the standard ML analysis on the entire data set using the Science Tools package. We used the `gtselect` tool to apply the cuts suggested by the *Fermi*-LAT collaboration for point-like sources² to minimize the impact of the systematics and the contamination from non-photon events. The Region of Interest (ROI), with a radius of 10° , was centred at the MST cluster centroid coordinates and the

photons were extracted with energies higher than 3 GeV applying the `P8SOURCE_V6` event class selection and the corresponding Instrument Response Functions. In the analysis, we considered all the 3FGL sources within the ROI from the cluster centroid, as well as the Galactic and extragalactic diffuse emission. Furthermore, a source with a power-law spectral distribution was assumed at the MST coordinates. The normalization of the 3FGL sources with $TS > 25$ within the ROI was allowed to vary in the fitting, while the parameters of the sources with $TS < 25$ were fixed to their catalogue values. The results are reported in Table 3.

In addition, we performed a simple photometry following the standard *Fermi*-LAT Aperture Photometry procedure³ in order to

² http://fermi.gsfc.nasa.gov/ssc/data/analysis/LAT_caveats.html

³ http://fermi.gsfc.nasa.gov/ssc/data/analysis/scitools/aperture_photometry.html

Table 2. Magnitude M values of the cluster MST 1945–2143 in three time intervals and with the two lower energy thresholds $E > 3$ GeV and $E > 10$ GeV.

Time interval	$E > 3$ GeV	$E > 10$ GeV
I	35.66	31.75
II	23.47	8.20
III	234.10	226.22

Table 3. Results of the ML analysis for the two clusters. The photon flux is in units of 10^{-10} ph cm $^{-2}$ s $^{-1}$.

	MST 0757–3728	MST 1945–2143
TS	51.76	185.53
Flux ($E > 3$ GeV)	1.3 ± 0.5	2.6 ± 0.4
Photon index	1.8 ± 0.6	2.2 ± 0.2

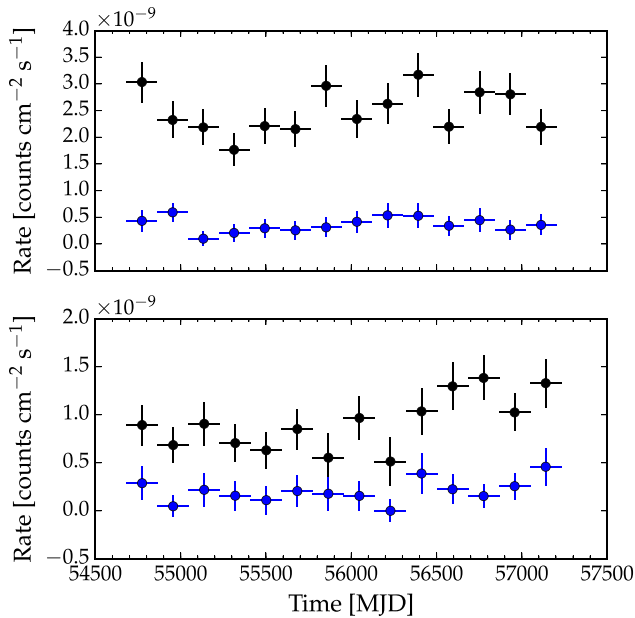


Figure 2. Aperture photometry LC of the photons at energy higher than 3 (black points) and 10 GeV (blue points) for MST 0757–3728 (upper panel) and 2FHL J1944.9–2144 (lower panel). Time binning is 6 months.

inspect a possible variability in the long-term LC of the source. Fig. 2 shows the resulting 6-month binned LC for the entire period (2008 August 04–2014 August 04) in the 3–300 and 10–300 GeV energy bands, obtained selecting events within 1° aperture radius. No model source has been assumed. In agreement with the MST analysis (Table 2), the 2FHL J1944.9–2144 source was brighter in the last period, while for MST 0757–3728, a shallow minimum of emission could have occurred around MJD ~ 55400 .

5 THE SEARCH FOR POSSIBLE COUNTERPARTS

5.1 The cluster MST 0757–3728

Considering that the γ -ray source coordinates above 10 GeV are given with an accuracy of a few arcminutes, we searched for possible counterparts within a cone of radius of 6 arcmin centred at the source

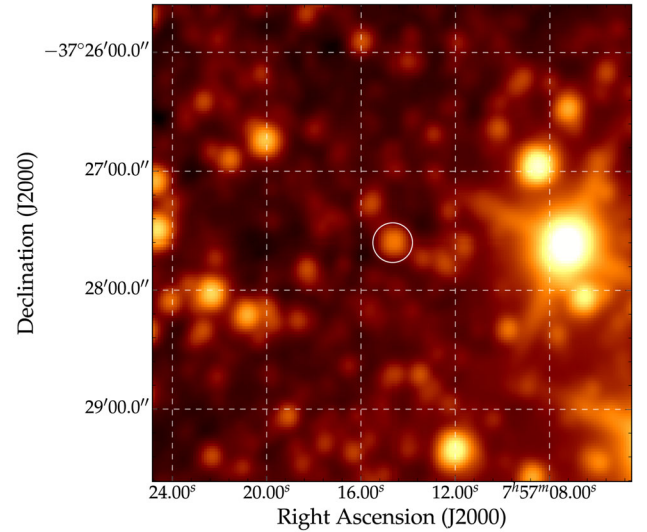


Figure 3. WISE image in the W1 ($3.4 \mu\text{m}$) bandpass with the likely infrared counterpart to the radio source NVSS J075714–372734, indicated by the circle. Image side is 4 arcmin.

position using the ASDC sky explorer tool⁴ that allows us to take into account many catalogues.

There are only two NRAO VLA Sky Survey (NVSS) radio sources: one is quite weak (3 mJy) and without high-confidence counterparts in other bands. The much more interesting source NVSS J075714–372734 has a flux density of 79.2 mJy at 1.4 GHz. In the second epoch Molonglo Galactic Plane Survey (Murphy et al. 2007) at 0.843 GHz, the corresponding source is MGPS J075714–372737, with a flux density of 99.3 mJy, indicating that its radio spectrum is flat. Moreover, at the rather large angular separation of 1.8 arcmin, there is also a Parkes-MIT-NRAO (PMN) survey source with a flux density of 88 ± 10 mJy at 4.85 GHz, comparable to the previous data. This, if actually associated with the NVSS source, would confirm the flat spectrum.

At an angular distance of 2.1 arcsec, fully compatible with the NVSS resolution, there is a very faint optical object in the European Southern Observatory DSS2-red image with very uncertain USNO photometric data. This source, however, is positionally consistent with a brighter mid-IR source AllWISE J075714.66–372736.0 in the *Wide-field Infrared Survey Explorer*⁵ (WISE; Wright et al. 2010), detected in all the four bandpasses with the following magnitudes: $[3.4] \mu\text{m} = (13.435 \pm 0.026)$ mag, $[4.6] \mu\text{m} = (12.625 \pm 0.024)$ mag, $[12] \mu\text{m} = (10.303 \pm 0.059)$ mag, $[22] \mu\text{m} = (8.683 \pm 0.348)$ mag. The WISE image in the $[3.4] \mu\text{m}$ band is given in Fig. 3. In the $[3.4]$ – $[4.6]$ – $[12] \mu\text{m}$ colour–colour diagram, these IR colours are consistent with those typical of a High-synchrotron-peaked BL Lac (HBL) as described in Massaro et al. (2011) for the tera electron volt BL Lac objects. This source is also included in the WISE Blazar-like Radio-Loud Source catalogue (D’Abrusco et al. 2014) as a class C (candidate) blazar. Optical spectroscopy of this source is not available and therefore we cannot safely establish whether it is a BL Lac object or an Flat Spectrum Radio Quasar (FSRQ); nevertheless, its blazar nature appears well-established and therefore it must be considered as the most interesting candidate for the counterpart of our new source.

⁴ <http://www.asdc.asi.it/>

⁵ <http://wise2.ipac.caltech.edu/docs/release/allsky/>

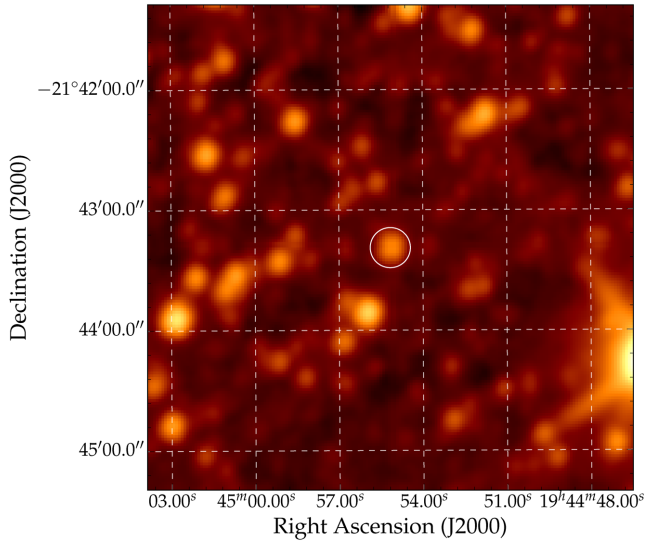


Figure 4. *WISE* image in the W1 bandpass ($3.4 \mu\text{m}$) of the region with the likely counterpart to the radio source NVSS J194455–214320, indicated by the circle. Image side is 4 arcmin.

5.2 The cluster MST 1945–2143/2FHL J1944.9–2144

In this case, five NVSS sources are found close enough to the cluster position, but the brightest and most interesting is NVSS J194455–214320 (Fig. 4) with a flux density at 1.4 GHz of 42.1 mJy, likely associated with the close X-ray source 1RXS J194455.3–214318. These sources are practically coincident with an optical object with GSC 2.2 magnitudes $B = 18.41$ mag and $R = 17.93$ mag. We found only one other radio measurement of this source in the Westerbork in the Southern Hemisphere catalogue (De Breuck et al. 2002) and its flux density at 0.352 GHz is 49 mJy, indicating a flat radio spectrum with a spectral index -0.12 ± 0.05 , corresponding to a spectral energy distribution (SED) exponent of 0.88 ± 0.05 : for this reason, it was included in the Low-Frequency Radio Catalog of Flat-Spectrum Sources catalogue (Massaro et al. 2014b) aimed at the identification of potential counterparts of γ -ray sources likely associated with blazars.

This source is also positionally well-consistent with the IR counterpart AllWISE J194455.16–214319.2, detected in all the four bandpasses with the following magnitudes: $[3.4] \mu\text{m} = (13.970 \pm 0.028)$ mag, $[4.6] \mu\text{m} = (13.377 \pm 0.034)$ mag, $[12] \mu\text{m} = (11.260 \pm 0.185)$ mag, $[22] \mu\text{m} = (8.755 \pm 0.491)$ mag. As for the previous cluster, the corresponding point in the $[3.4]$ – $[4.6]$ – $[12] \mu\text{m}$ colour–colour diagram is consistent with an HBL as described in Massaro et al. (2011) for the TeV BL Lac objects.

There is a good quality optical spectrum available from the 6dF data base (Jones et al. 2009), here reported in Fig. 5: surprisingly, it has a clear stellar appearance with well-defined Balmer lines with the exception of the $H\alpha$ and it is classified as a DA white dwarf.

5.3 The SEDs

Using the good photometric data available from literature and data bases, we built the SEDs of both γ -ray sources and their possible counterparts. The resulting plots are presented in the two panels of Fig. 6: the two SEDs are remarkably similar to that of a typical HSP source (see, for instance, Giommi et al. 2012). We fitted a log-parabola:

$$S(E) = AE^{-a-\beta \text{Log}E} \quad (1)$$

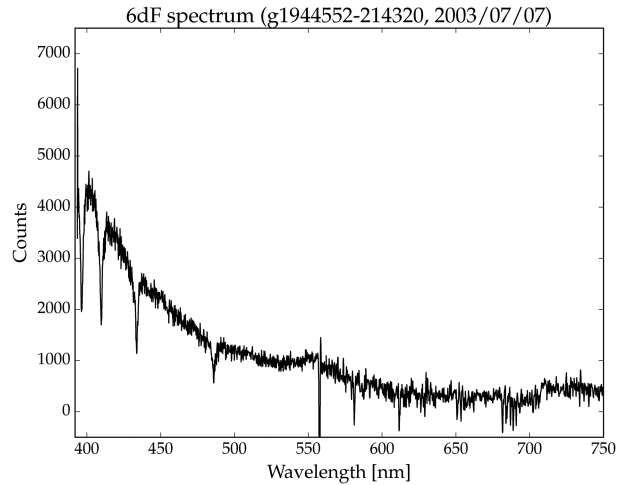


Figure 5. The 6dF spectrum of the possible optical counterpart to NVSS J194455–214320: note the absorption lines of the Balmer series.

to data from the IR to the UV/X-ray range to estimate the frequency of the synchrotron bump and obtained $\approx 10^{15}$ Hz and $\approx 5 \times 10^{15}$ Hz for MST 0757–3728 and 2FHL J1944.9–2144, respectively. Also, the curvature parameter β resulted equal to 0.16 and 0.20, values frequently found for blazars. In Fig. 6 is also shown a linear fit $S(E) = KE^{-\alpha r}$, carried out considering only the radio data up to the frequencies corresponding to the AllWISE filters. For 2FHL J1944.9–2144, the different slope with respect to the one given by radio data alone is due to the constraint of matching the mid-IR data.

6 SUMMARY AND DISCUSSION

The high-energy γ -ray sky, according to the new scenario derived from *Fermi*-LAT observations, appears characterized by the presence of several thousands of sources, many of which are variable over different time-scales (Massaro, Thompson & Ferrara 2016). The improvement in the data quality reached with the Pass 8 release and the continuous enrichment due to the extension of the *Fermi*-LAT sky monitoring make possible the detection of new interesting sources. In this paper, we report the discovery of two γ -ray sources with high significance: one in a region close to the Galactic equator and the other having an incongruous possible counterpart.

The time and spectral behaviour of MST 0757–3728 in the γ -ray band appear blazar-like and therefore we are confident about the proposed counterpart; we cannot safely establish, however, whether it is a BL Lac object or an FSRQ because of the lack of optical spectroscopy. Radio and γ -ray spectra are suggestive of a quasar, while the IR *WISE* colours are those of an HBL source.

The characteristics of the proposed counterpart to 2FHL J1944.9–2144, and particularly its optical spectrum, are quite unusual. White dwarf DA stars, in fact, are neither known as flat spectrum radio sources nor as γ -ray emitters. Cross-matching a sample of 14120 DA-type stars from the SDSS DR7 WD catalogue (Kleinman et al. 2013) with the 3FGL catalogue within a 6 arcmin angular distance, resulted in only 25 of them possibly associated with γ -ray sources: 22 of which with a counterpart in the RomBZCAT (5th Edition; Massaro et al. 2014a, 2015) blazar catalogue and the remaining three close to CRATES (Healey et al. 2007) radio sources and therefore likely associated with other blazars not yet optically identified.

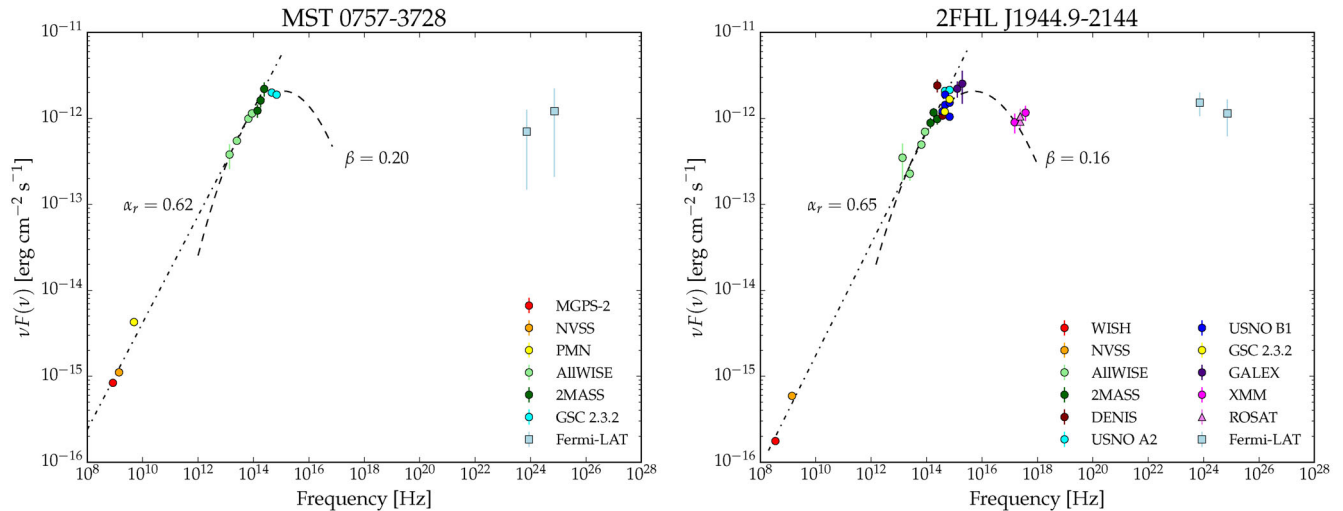


Figure 6. The SED of MST 0757–3728 (left-hand panel) and of 2FHL J1944.9–2144 (right-hand panel).

The possibility that this object can be considered as an NS-WD binary, as in the case of the recently discovered millisecond pulsar (MSP) PSR J1824+10 in the error box of 3FGL J1824.0+1017 (Cromartie et al. 2016), cannot be excluded. Even the occurrence of a flat radio spectrum below 1 GHz does not rule out this possibility because, although rare, it is observed in a few MSPs (Kondratiev et al. 2016). However, some alternatives must be taken into account: the possibility, although quite rare, that the close angular separation between a blazar and a brighter WD might be due to chance or the fact that the reported 6dF spectrum does not correspond to the optical object. We asked the 6dF data management to verify that the coordinates of their pointing (RA = 19^h44^m55^s.16, Dec. = −21°43′19″.5; Read, private communication) were correctly reported and obtained a confirmation. The only way to disentangle this unusual finding is to perform new and more accurate astrometric and spectroscopic observations of this puzzling object.

ACKNOWLEDGEMENTS

Part of this work is based on archival data, software or online services provided by the ASI Science Data Center (ASDC). We furthermore acknowledge use of archival *Fermi*-LAT data, of the Final Release 6dFGS archive and of the SDSS and DSS archives. We are particularly grateful to Mike A. Read of the 6dF team.

REFERENCES

Abdo A. A. et al., 2010, *ApJS*, 188, 405
 Abdo A. A. et al., 2013, *ApJS*, 208, 17
 Acero F. et al., 2015, *ApJS*, 218, 23
 Acero F. et al., 2016, *ApJS*, 224, 8
 Ackermann M. et al., 2013, *ApJS*, 209, 34
 Ackermann M. et al., 2016, *ApJS*, 222, 5
 Atwood W. B. et al., 2009, *ApJ*, 697, 1071
 Campana R., Massaro E., Gasparrini D., Cutini S., Tramacere A., 2008, *MNRAS*, 383, 1166

Campana R., Bernieri E., Massaro E., Tinebra F., Tosti G., 2013, *Ap&SS*, 347, 169
 Campana R., Massaro E., Bernieri E., D’Amato Q., 2015, *Ap&SS*, 360, 19
 Campana R., Massaro E., Bernieri E., 2016a, *Ap&SS*, 361, 183
 Campana R., Massaro E., Bernieri E., 2016b, *Ap&SS*, 361, 185
 Campana R., Massaro E., Bernieri E., 2016c, *Ap&SS*, 361, 367
 Cromartie H. T. et al., 2016, *ApJ*, 819, 34
 D’Abrusco R., Massaro F., Paggi A., Smith H. A., Masetti N., Landoni M., Tosti G., 2014, *ApJS*, 215, 14
 De Brueck C., Tang Y., de Bruyn A. G., Röttgering H., van Breugel W., 2002, *A&A*, 394, 59
 Giommi P. et al., 2012, *A&A*, 541, A160
 Healey S. E., Romani R. W., Taylor G. B., Sadler E. M., Ricci R., Murphy T., Ulvestad J. S., Winn J. N., 2007, *ApJS*, 171, 61
 Jones D. H. et al., 2009, *MNRAS*, 399, 683
 Kleinman S. J. et al., 2013, *ApJS*, 204, 5
 Kondratiev V. I. et al., 2016, *A&A*, 585, A128
 Massaro E., Tinebra F., Campana R., Tosti G., 2009, preprint ([arXiv:0912.3843](https://arxiv.org/abs/0912.3843))
 Massaro F., D’Abrusco R., Ajello M., Grindlay J. E., Smith H. A., 2011, *ApJ*, 740, L48
 Massaro E., Marchegiani P., Perri M., Giommi P., Piranomonte S., 2014a, in Massaro E., Maselli A., Leto C., Marchegiani P., Perri M., Giommi P., Piranomonte S., eds, *Multifrequency Catalogue of Blazars*, 5th edn. Aracne Editrice, Rome, Italy
 Massaro F., Giroletti M., D’Abrusco R., Masetti N., Paggi A., Cowperthwaite P. S., Tosti G., Funk S., 2014b, *ApJS*, 213, 3
 Massaro E., Maselli A., Leto C., Marchegiani P., Perri M., Giommi P., Piranomonte S., 2015, *Ap&SS*, 357, 75
 Massaro F., Thompson D. J., Ferrara E. C., 2016, *A&AR*, 24, 2
 Mattox J. R. et al., 1996, *ApJ*, 461, 396
 Murphy T., Mauch T., Green A., Hunstead R. W., Piestrzynska B., Kels A. P., Sztajer P., 2007, *MNRAS*, 382, 382
 Nolan P. L. et al., 2012, *ApJS*, 199, 31
 Wright E. L. et al., 2010, *AJ*, 140, 1868

This paper has been typeset from a $\text{\TeX}/\text{\LaTeX}$ file prepared by the author.